Beam tests of a CCD sensor for vertex detector at JLC

T. Aso [a,1], S. Takahasi [b], N. Tamura [b], S. Komaji [c], T. Kuniya [c], T. Miyahara [c], K. Nakamura [c], K. D. Stefanov [c], T. Tsukamoto [c], H. Watanabe [c], Y. Shirasaki [d], H. Sumiya [d], T. Nagamine [d], K. Abe [d], A. Miyamoto [e], Y. Sugimoto [e],

[a] *Department of Computer engineering, Toyama National College of Maritime Technology, Toyama 933-0293, Japan*

[b] *Department of Physics, Niigata University, Niigata 950-2181, Japan*

[c] *Department of Physics, Saga University, Saga 840-8502, Japan*

[d] *Department of Physics, Tohoku University, Miyagi 980-8578, Japan*

[e] *High Energy Accelerator Research Organization (KEK), Ibaraki 305-0801, Japan*

Abstract

We have examined the performance of CCD sensors at room temperature for use as a micro vertex tracker in a future linear collider experiment, JLC. A test tracker which consists of 4 layers of CCDs was exposed to minimum ionizing particles at KEK PS. The spatial resolution of the three different type of CCDs were measured at temperature of $-15°$C and $+5°$C. The minimum ionizing signals were detected with sufficient signal-to-noise ratio (>10) and excellent spatial resolution (< 4 μm), even at $+5°$C.

1 Introduction

The Joint Linear Collider (JLC) project[1] consists of the construction of a linear collider and the experiments therewith, at an initial center of mass energy around 250 GeV which will eventually reach TeV region.

[1] Corresponding author.
Tel: +81 766 86 5275
Fax: +81 766 86 5110
E-mail: aso@toyama-cmt.ac.jp

As the energy increases, particles in a jet become more and more collimated. CCD (Charge Coupled Device) is one of the best candidates for a vertex detector in the JLC detector. Since, in contrast to silicon strip detectors, CCD has unambiguous reconstruction capability by 2-dimmensional array of pixels, higher track densities and backgrounds can be tolerated and pattern recognition is more efficient. The CCDs will be operated at close to room temperature in order to reduce the amount of materials for the cooling system between the vertex detector and the central tracking detector.

In general, it is desirable to run the CCDs at low temperature of approximately 180°K[2], in order to suppress dark currents and minimize the effects of radiation damage, At higher temperature, the performance of CCDs is deteriorated by thermally generated background signal, i.e. dark current. Its statistical fluctuation could be a serious source of noise in the detection of minimum ionizing particles. Recently, a novel method called as Multi Pinned Phase (MPP) operation[3] is proposed to suppress the dark current. In the MPP mode, the array clocks are biased sufficiently negative to invert all phases and the surface potential is "pinned" to substrate potential. As a result, the thermal excitation of electrons is extremely suppressed. It reduces the dark current by a factor of 20 compared with normal non-inverted operation mode.

In this paper, we report a study on the properties of CCDs in MPP operation by detecting minimum ionizing particles at room temperature . The results are presented in terms of signal-to-noise ratios (S/N) and spatial resolutions as a function of temperature.

2 Experiment

Three kinds of CCD detectors in MPP operation were used in the experiments. Table 1 is a list of the test samples with important parameters. Two of the three CCDs were S5466 fabricated by Hamamatsu Photonics K.K.[4] (HPK) , but with different depth of epitaxial layers, 10μm (HPK10) and 50μm (HPK50), respectively. Those consists of 512 $\times$ 512 pixels and the pixel size is 24 μm $\times$ 24 μm. Another one was CCD02-06 fabricated by EEV Company[5]. The CCD02-06 consists of 385 $\times$ 578 pixels and the pixel size is 22 μm $\times$ 22 μm. It has epitaxial depth of 20μm (EEV).

A CCD tracker was set up at the T1 test beam line of the 12-GeV proton synchrotron (PS) at High Energy Accelerator Research Organization (KEK) as shown in Fig.1. The negative pion beam was used in the experiment. The momentum of the beam was chosen to be 2.0 GeV/c, 1.0 GeV/c, 0.7 GeV/c, and 0.5 GeV/c. The normal axis of the CCD tracker was aligned to the beam. The tracker consisted of four layers of CCDs as shown in the figure. Two

reference CCD detectors were located upstream of the test sample, for precise reconstruction of a particle track. Al_2O_3 supporting substrate behind the CCD was removed from the reference CCD in the second layer to minimize the multiple-scattering effect. Another CCD was located at the end of the tracker, for the reduction of accidental tracks. The reference CCDs were HPK/S5466 with epitaxial depth of 10μm. All of the CCDs were driven at a rate of 250 kpixels/s, and operated in a full-frame readout mode. Readout cycle was 3 s to synchronize with the PS cycle. Integration time was about 1.7 s except reading time. The tracker was enclosed in a constant temperature and humidity chamber together with the driving circuits.

3 Results

3.1 Signal to Noise ratio

The charge created by a penetrating particle is collected generally by several consecutive pixels, which form a cluster. In order to find the cluster, we first look for a leading pixel whose charge is higher than the threshold and is highest in the region. The threshold was defined as 7$\sim$15 times of the noise level. The threshold was detemined to reduce the noise contribution keeping the efficiency good. Total charge of the cluster is sum of the charges of the leading pixel and neighboring pixels. Fig.2 shows a typical event of a minimum ionizing particle which was detected in HPK10. Fig.3 shows clustering size dependence of the total charge, where clustering size is defined as N$\times$N pixels. As shown in the figure, all the deposited charges are collected in the cluster size of 2$\times$2 pixels for HPK10 and EEV. For HPK50, however, more than 5$\times$5 pixels are neccesary to collect all of the deposited charges. Approximately 920 electrons/10μm[6] is expected to be produced by a minimum ionizing particle in silicon, which is consistent with the observed charge by taking into account the depth of epitaxial layers.

We chose clustering size of 2$\times$2 pixels for both determination of the position and evaluation of the S/N values. Fig. 4 shows the dependence of S/N, which is defined as the division of the most probable value of the collected charge by the noise, at the temperature. As temperature is raised, the S/N for HPK CCDs significantly degraded due to the increase of the dark current, while the S/N was almost unchanged for EEV in the range from -15°C to $+15^{\circ}$C. This is because the noise caused by the dark current is not a dominant source in the total noise for EEV. The main source is considered to be an external noise which comes from a cooling system. The degradation of the S/N for HPK50 in this range was larger than that for HPK10, since the dark current for HPK50 increases more rapidly than that for HPK10 as temperature rises.

In the previous paper[7], the operational condition at higher temperature was discussed with the dependence of dark current on temperature and readout drive frequency. When CCD is driven at faster rate, the noise due to dark current is suppressed. Then, the S/N values are expected to improve.

3.2 Spatial resolution

First of all, the position of the cluster was determined using the 2×2 pixels for computing the hit position of the particle passing through the detector. We adopted two ways of determination. One is the Analog-Centroid-Method (AC-method)[9], where the position is calculated as the charge weighted average of the four pixels. Another is the Ratio-Location-Mapping-Method (RLM-method). In the RLM-method, the relation between the position $x(y)$ of the cluster and the charge ratio $R_{x(y)}$ of adjacent pixel in $x(y)$ direction($Q_{x(y)}$) to the leading pixel(Q_{max}), i.e. $R_{x(y)} = Q_{x(y)}/Q_{max}$, was derived from the data(Fig. 5), where $x(y)$ was calculated by extrapolating the track from the upstream reference CCDs. In the figure, the x is normalized by the pixel pitch so that the $x = 0$ corresponds to the center of the leading pixel, while $x = 0.5$ corresponds to the middle point of the gap between two pixels in x direction. The RLM function was obtained by fitting to the data. The position of the cluster was then calculated from obtained charge ratio by using the RLM function. The RLM function represents a spread of charges produced by incident particle. For example, if a particle hits the position x=0.3, the charge sharing to the adjacent pixel is about 8%, 13%, and 25% of the leading pixel, for EEV, HPK10, and HPK50, respectively. HPK50 has more spread signal than HPK10, since the epitaxial depth of HPK50 is larger than that of HPK10. The charge sharing of EEV is smallest among all samples. This reason is considered to be that the EEV has different structure from HPK type of CCDs.

In the AC-method, the linear relation between the position of the cluster and the charge ratio of the four pixels is assumed. However, the relation between $R_{x(y)}$ and $x(y)$ is not linear as shown in Fig.5. Therefore, we can not obtain the best position resolution by using the AC-method.

The spatial resolution was derived from the residual distributions, which is the deviation of the cluster in the test sample from the extrapolated hit position from the upstream reference CCDs. The residual resolution ($\sigma_{residual}$) was obtained by fitting this distribution with the Gaussian distribution. The $\sigma_{residual}$ contains the contributions from multiple Coulomb scattering (MCS) and the finite resolution of the reference CCDs. The MCS effect was subtracted by deriving the residual resolution at infinite momentum. The type of reference CCDs were same as HPK10 so that the resolution of HPK10 was obtained.

by assuming same spatial resolution for those HPK10s.

The obtained spatial resolutions for normal incidence are listed in Table 2, for AC-method and RLM-method, respectively. At -15°C, the spatial resolutions for HPK10 and EEV were improved about 20% by taking account the non-linear charge sharing characteristics by RLM-method. When the temperature was raised from -15°C to $+5$°C, the spatial resolutions obtained by using RLM-method were changed its values according to the variation of the S/N value, i.e. about 20% worse for HPK10, and almost unchanged for EEV. On the other hand, the spatial resolutions derived from AC-method were almost same, even if the temperature was changed from -15°C to $+5$°C. Since the charge sharing is small in adjacent pixels for HPK10 and EEV, the resolution of R_x is deteriorated by the noise. This is the reason why RLM-method is more sensitive to the S/N value than AC-method. This conjecture explains the temperature dependence for HPK10 and EEV as well. For HPK50, the spatial resolutions obtained by RLM-method and AC-method were almost same value at both of -15°C and $+5$°C. The spatial resolution become worsened about 30% if the temperature was raised from -15°C to $+5$°C. This is caused by the 50% degradation of S/N ratio.

Efficiency was measured by looking for the existence of associated cluster in the interpolated region on the test sample, for the tracks which have a cluster in three reference CCDs. Efficiencies at -15°C for 2 GeV pions were $98.8^{+1.2}_{-1.5}$%, $99.4^{+0.6}_{-1.6}$%, and $97.8^{+2.2}_{-1.6}$%, for HPK10, HPK50, and EEV, respectively.

4 Summary

We have studied the performance of a CCD tracker using pions at the 12 GeV PS at KEK. Three types of CCD detectors which have different structures were tested.

The present series of test showed that: 1)S/N ratio of more than 10 can be achieved even at $+5$°C by successful operation in the MPP mode; 2) The spatial resolutions were improved for HPK10 and EEV by taking the nonlinear charge sharing characteristics into account by RLM-method; 3) The temperature dependence of the spatial resolution in AC-method was small for HPK10 and EEV samples, while spatial resolution become worse about 30% if the temperature was changed from -15°C to $+5$°C for HPK50.

We have measured the spatial resolution of CCDs in MPP operation for minimum ionizing particles. All of the three types of CCDs showed S/N > 10 and the excellent spatial resolution of < 4 μm, even at $+5$°C, which satisies the requirements of the JLC project.

Acknowledgements

This work is supported in part by KEK Joint Research and Development Program, JSPS Japanese-German Corporation Program, and Grant-in-Aid for Scientific Research of the Ministry Education, Science and Culture.

References

[1] JLC group, JLC *KEK Report* **92-16** (1992).

[2] J.E. Brau et al., *IEEE Trans.Nucl.Sci.* **43** (1996) 1107–1112.

[3] J. Janesick et al., *SPIE. Optical Sensors and Electric Photography* **1071** (1997) 153. in: N. S. Saks. *IEEE Electron Device Lett.* **EDL-1-7** (1980) 131.

[4] S5466, *FFT-CCD Image Sensor S5466.* (1995) Hamamatsu Photonics K.K. Ltd.

[5] CCD02-06 Series SIS, *A1A-CCD02-06 Series Scientific Image Sensor Issue 4.* (1993) EEV Co. Ltd.

[6] C. White, *Nucl. Instr. and Meth.* **A351** (1994) 217.

[7] T. Tsukamoto et al., *Nucl. Instr. and Meth.* **A383** (1996) 256. in: T. Tsukamoto et al., *KEK Preprint.* **98-19** (1998).

[8] R. Turchetta, *Nucl. Instr. and Meth.* **A335** (1993) 44.

Table 1
Test Samples.

Test sample	CCD type	Image area [mm]	Pixel pitch [μm]	Pixel format (H×V)	Epitaxial layer [μm]	Amplifier sensitivity [μV/e]
HPK10	S5466	12.29×12.29	24×24	512×512	10	2.0
HPK50	S5466(Special)	12.29×12.29	24×24	512×512	50	2.0
EEV	CCD02-06	8.5×12.7	22×22	385×578	20	1.0

Table 2
Spatial resolution in μm.

Temperature	Method	HPK10	HPK50	EEV
−15°C	AC	3.56±0.02	2.67±0.09	3.71±0.08
	RLM	2.76±0.03	2.79±0.09	2.94±0.10
+5°C	AC	3.68±0.03	3.34±0.10	3.84±0.08
	RLM	3.46±0.04	3.67±0.12	2.59±0.16

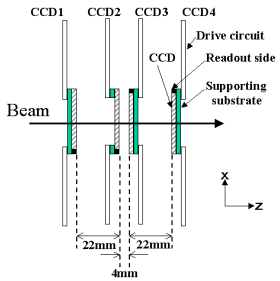

Fig. 1. Schematic view of the setup. Both CCD1 and CCD2 were reference CCDs for tracking. CCD3 was the test sample. CCD4 was used for reduction of the accidental tracks, and the measurement of the efficiency.

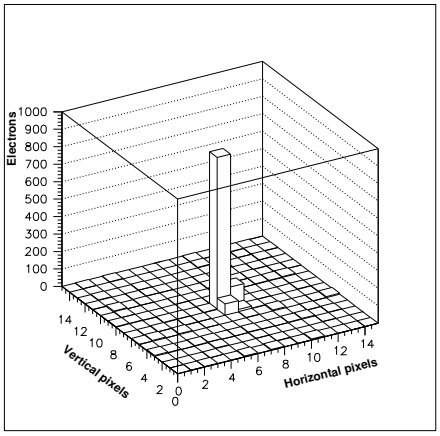

Fig. 2. Typical event by a minimum ionizing particle detected in HPK10, where the height is a collected charge in the unit of electrons after the correction of the sensitivity of the detector including the gain of the amplifier.

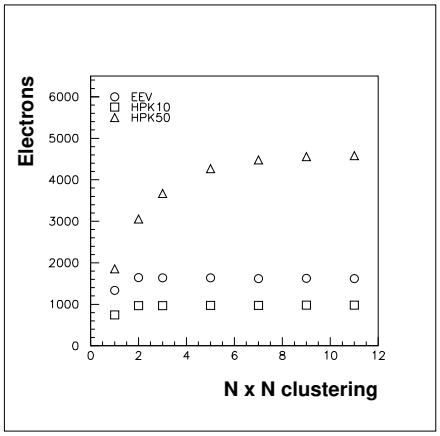

Fig. 3. Collected charge for a minimum ionizing particle as a function of clustering size, where clustering size was defined as N×N pixels. The horizontal axis represents a number of N and vertical axis is a collected charge in the unit of electrons after the correction of the sensitivity of the detector including the gain of the amplifier.

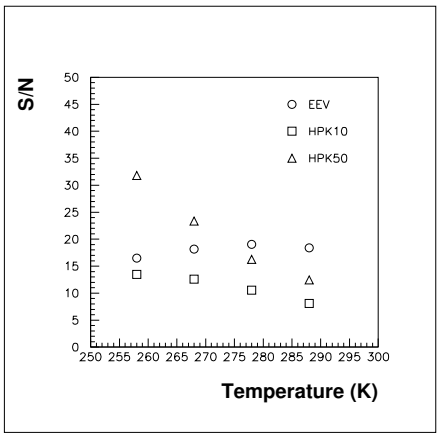

Fig. 4. Signal-to-Noise ratio as a function of temperature.

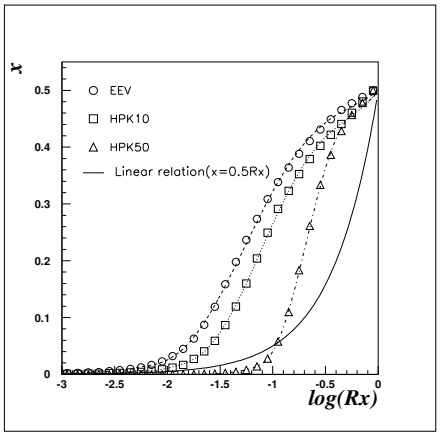

Fig. 5. The relation of the position x of the cluster with the charge ratio R_x of the maximum charge to the charge in the adjacent pixel, where x is the position of the cluster normalized by pixel pitch. Solid line represents a linear relation between x and R_x. The other Lines are obtained from the fit to data.